THE JOURNAL OF PHYSICAL CHEMISTRY B

 VOLUME 107, NUMBER 12, MARCH 27, 2003

LETTERS

Large-Scale Organizations of MoO_3 Nanoplatelets with Single-Crystalline $MoO_3(4,4'\text{-bipyridyl})_{0.5}$

Xu Ming Wei and Hua Chun Zeng*

Department of Chemical and Environmental Engineering, Faculty of Engineering, National University of Singapore, 10 Kent Ridge Crescent, Singapore 119260

Received: November 9, 2002; In Final Form: January 26, 2003

We report a novel assembly approach for fabrication of molybdenum trioxide nanoplatelets with precise controls of stack architecture and crystallographic phase (either β-MoO_3 or α-MoO_3, or their mixture) at 300−450 °C. The self-assembly of these metal oxides occurs within a predefined space of original hybrid single-crystals (i.e., the assemblies have a dimension as large as 50−250 μm), and an overall oxide assembly is strictly integrated throughout the original crystal space provided. In this sense, each single-crystal of the hybrid precursor can be viewed as a microscopic "green compact" analogous to the macroscopic one in ceramic processing.

In recent years, fabrication of nanostructured metal oxides and hydroxides has become an active research area in low dimensional materials synthesis.[1−4] At the present time, most of morphological organizations of metal oxides and other nanostructures are focused on surfactant-assisted self-assembly in liquid phase at low or moderate temperatures. To make these materials usable in high-temperature applications, nonetheless, large-scale organizing metal-oxide nanostructures in a desired manner at elevated temperatures is particularly challenging, due to difficulties in controlling interconnectivity among individual crystallites, random nucleation, and grain growth upon heat-treatment. Using inorganic−organic hybrid solid precursors, for example, mesoporous molecular-sieve type materials (e.g., MCM-41) have been prepared by "massive templates" formed with organic surfactant micelles.[2] Recently, layered inorganic−organic hybrids had been utilized for syntheses of one-dimensional (1D) discrete crystallites nanorods and nanotubes under hydrothermal conditions and subsequent thermal treatments with or without elimination of the organic intercalants (such as amines with long alkyl chains).[4] In this letter, we will report a novel synthetic approach for both synthesis and organization of nanostructured metal-oxide platelets using inorganic−organic hybrid precursors through control of heating routines. More specifically, molybdenum trioxide nanoplatelets have been prepared with desired stack-architecture and crystallographic phase (either β-MoO_3 or α-MoO_3, or their mixture) at 300−450 °C. This method includes an intercalation of inorganic macromolecular sheets of MoO_3 with an organic spacer 4,4′-bipyridine, elimination of this bidentate spacer, and oriented sheet-condensation under air or nitrogen at elevated temperatures, as depicted in Figure 1. The resultant 2D nanostructures are self-organized into a 3D stack, showing distinct inter-crystallite relationships. Furthermore, final platelet stacks preserve the original crystal morphology of the starting $MoO_3(4,4'\text{-bipyridyl})_{0.5}$, i.e., the oriented organization of MoO_3 nanoplatelets takes place according to the space provided by the pristine single-crystal precursors. Thus, the role of "green compact"[5] of this inorganic−organic layered hybrid for organized nanooxide synthesis is demonstrated.

The investigation was started with synthesis of $MoO_3(4,4'\text{-bipyridyl})_{0.5}$ single-crystals.[6,7] Hydrothermal reactions were conducted at 150 °C for 72 h using α-MoO_3 (0.12 g, Aldrich,

* To whom correspondence should be addressed. E-mail: chezhc@nus.edu.sg.

10.1021/jp0274177 CCC: $25.00
Published on Web 02/28/2003

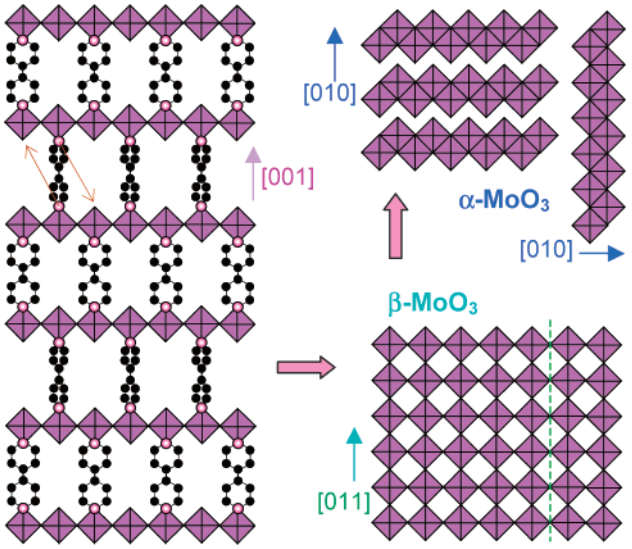

Figure 1. Schematic illustration of MoO_3 molecular sheet condensation processes. MoO_6 octahedra are represented by purple squares. Carbon and nitrogen atoms of 4,4′-bipyridine spacer are indicated with black and red round dots, respectively. Red arrows indicate the matching points in sheet condensation. Both β-MoO_3 and α-MoO_3 structures are viewed along [100] axis.

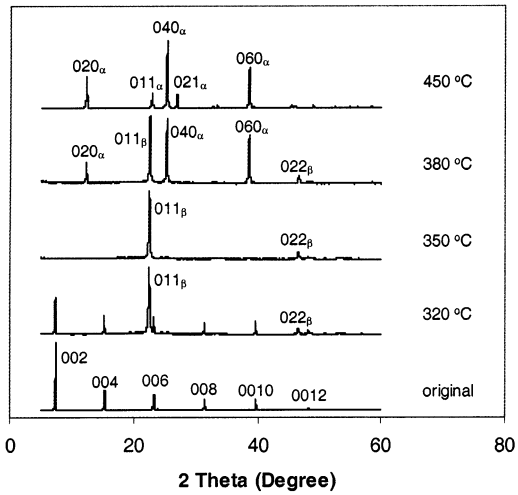

Figure 2. Powder XRD patterns (intensity in arbitrary unit) of samples of $MoO_3(4,4'\text{-bipyridyl})_{0.5}$ crystals (names "original") heated in laboratory air at various temperatures: 320, 350, 380, and 450 °C. The heating temperature was preset to 300 °C (except for 320 °C-experiment at 270 °C) for 1 h (at rising rate 5 °C/min), followed by heat-treatments at 320, 350, 380, and 450 °C, respectively, for 2 h (at rising rate 0.1 °C/min).

> 99.5%), 4,4′-bipyridine (0.13 g, $C_{10}H_8N_2$, Fluka, > 99%), and deionized water (15 g) in a Teflon lined stainless autoclave. The yellowish $MoO_3(4,4'\text{-bipyridyl})_{0.5}$ single-crystals were then washed with deionized water and dried at room temperature. Within these single-crystalline "green compacts", the MoO_3 molecular sheet condensation was controlled with oxidative (laboratory air) or inert atmosphere (pure nitrogen, flow rate = 30 mL min^{-1}) with various heating routines. To have a deeper understanding of interactions between organic and inorganic interphases upon the firing processes, the prepared products were characterized with XRD (Shimadzu XRD-6000), SEM (JEOL, JSM-5600LV), and FTIR (Bio-Rad FTS-135).

As illustrated in Figures 1 and 2, the starting compound, $MoO_3(4,4'\text{-bipyridyl})_{0.5}$, belongs to monoclinic symmetry and has a basal spacing of 1.12 nm ($d_{002} = c/2$).[6,7] The layered structure of this hybrid material is clearly indicated in the (00*l*) reflections (Figure 2), in which 4,4′-bipyridine ligands bond coordinately with central molybdenum, resulting in heteroatomic octahedra (MoO_5N) that interconnect with each other via four coplanar oxygen atoms.

Our XRD/FTIR studies indicate that deintercalation of 4,4′-bipyridne occurs upon thermal treatments (see FTIR results in Supporting Information). This process can be divided into two discrete steps: $MoO_3(4,4'\text{-bipyridyl})_{0.5} \rightarrow \beta\text{-}MoO_3 \rightarrow \alpha\text{-}MoO_3$. The metastable β-MoO_3 phase (monoclinic, SG: $P2_1/c$, a = 0.7122 nm, b = 0.5374 nm and c = 0.5565 nm; or viewed as pseudo-cubic, similar to ReO_3)[8] is formed at 320−350 °C in air. As revealed in Figure 3a, the resultant MoO_3 shows layered crystal strips and elongated voids (generated by deintercalation of 4,4′-bipyridine) parallel to the (001) crystal surface of MoO_3-$(4,4'\text{-bipyridyl})_{0.5}$. The thickness of crystal strips is in the range of 80−220 nm, with vertical interconnection among them. Since XRD pattern shows only 0*kk* reflections (011 and 022) for this sample (Figure 2), it is known that [011] is the preferred orientation for these layered strips. Relationships among the resultant crystal strips, void spaces, and the preferred crystallographic orientation reveal unambiguously that the MoO_3 molecular sheet condensation is responsible for the formation of β-MoO_3. Concerning the formation of β-MoO_3, it is noted that the removal of 4,4′-bipyridine will create oxygen vacancies between two neighboring MoO_3 sheets. A vertical topotactic condensation among the molecular sheets seems to be the most efficient, because the oxygen vacancies generated can be filled with molybdenyl bonds (Mo═O) from a neighboring sheet with only a minimum horizontal shift (red arrows; Figure 1).

At 380 °C, β-$MoO_3 \rightarrow$ α-MoO_3 (orthorhombic, SG: Pbnm, a = 0.3963 nm, b = 1.386 nm, c = 0.3696 nm; basal spacing $d_{010}/2 = b/2$)[9−11] transformation takes place in air, as shown in Figure 2 (380 °C pattern). After 2 h, ca. 50% of β-MoO_3 has been converted into α-MoO_3 based on relative XRD intensities of these two phases. Upon the formation of double-layered structure in α-MoO_3, the thickness of the crystal platelets is significantly reduced (60−100 nm) while the void space is increased (Figure 3b). Evidenced in pronounced 0*k*0 (α: 020, 040, and 060) and 0*kk* (β: 011 and 022) reflections (Figure 2), the MoO_3 platelets of both phases are preferentially stacked along [010] and [011] axes.[8] Since they are well interconnected, the orientated platelets can now be viewed as an integrated 3D nanostack. With a prolonged heating at 380 °C for 4 h, phase-pure α-MoO_3 platelets (not shown) can be obtained with an essentially same morphology as that of Figure 3c below.

Interestingly, more complex stack architectures can be further achieved. In Figure 3c, an orthorhombic assembly of α-MoO_3 platelets with different ⟨010⟩ orientations (inter-platelet angle 90°) is reported. The ⟨010⟩ oriented α-MoO_3 platelets are well faceted with {100} and {101} planes.[12] The β-MoO_3 is indeed an intermediate phase prior to α-MoO_3, as evidenced in the stacking along all ⟨011⟩ and ⟨100⟩ directions of β-MoO_3. Drastic changes or subtle modifications on stack architecture can still be obtained by varying heating routines. For example, unidirectional stacks of faceted α-MoO_3 nanoplatelets (rather than the 90°-intersected {010} platelets of Figure 3c) as thin as 40−60 nm in [010] have been prepared at 400 °C just with variation of heating rate (e.g., 0.2−1.0 °C/min, instead of 0.1 °C/min used in Figure 3c).

Compared to air, the conversions of $MoO_3(4,4'\text{-bipyridyl})_{0.5} \rightarrow \beta\text{-}MoO_3 \rightarrow$ α-MoO_3 proceed much slower in nitrogen ambience, as elucidated in the XRD investigation of Figure 4. For instance, α-MoO_3 forms only at 400−420 °C (compared

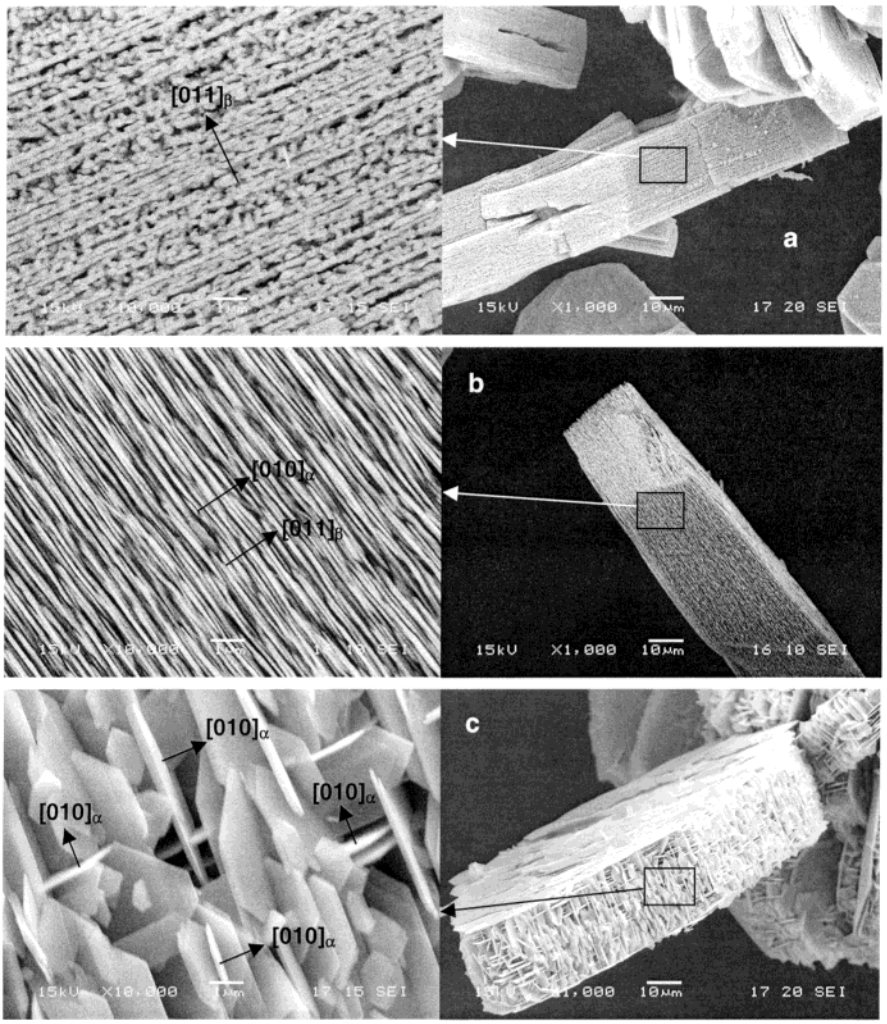

Figure 3. SEM images of detailed and overall MoO_3 platelets generated via heating MoO_3(4,4′-bipyridyl)$_{0.5}$ crystals in laboratory air: (a) phase pure β-MoO_3 stacks (5 °C/min to 300 °C for 1 h + 0.1 °C/min to 350 °C for 2 h), (b) mixed phase α-MoO_3 (∼50%) and β-MoO_3 (∼50%) stacks (5 °C/min to 300 °C for 1 h + 0.1 °C/min to 380 °C for 2 h), and (c) phase pure α-MoO_3 assembly (5 °C/min to 300 °C for 1 h + 0.1 °C/min to 400 °C for 2 h). Framed rectangles in the right-hand-side images indicate the respective examined areas in the overall MoO_3 platelet assemblies that preserve the original crystal shapes of MoO_3(4,4′-bipyridyl)$_{0.5}$. Refer to Figure 1 for further details.

to 380 °C in air). In this agreement, FTIR examination reveals that it is more efficient to remove 4,4′-bipyridine in air atmosphere than in nitrogen (4,4′-bipyridine can be completely depleted in air at ≤350 °C; see Supporting Information). Nonetheless, except for the temperature delay, the layered structures reported in Figure 3 can also be obtained in nitrogen; unidirectional phase-pure α-MoO_3 nanoplatelets thinner than 90 nm can be stacked along [010] at 420−450 °C (see Supporting Information).

In all the cases, it is believed that the nucleation of MoO_3 nanoplatelets starts on the topmost crystal surfaces. This is particularly illustrative in Figure 3c (inset) where the topmost (001) surface of MoO_3(4,4′-bipyridyl)$_{0.5}$ crystal becomes the (010) surface of α-MoO_3. From the above examples, it is important to realize that the integrity of final nanoarchitecture is well preserved, owing to an excellent interconnectivity generated among the crystal platelets. In this sense, the role of pristine MoO_3(4,4′-bipyridyl)$_{0.5}$ single-crystals is essentially similar to the "green compact" in ceramic materials processing, as overall dimensions of the assembled stacks can be predetermined by the crystal size of MoO_3(4,4′-bipyridyl)$_{0.5}$ which is in the range of 50−250 μm. By changing the length of organic pillars (e.g., bipyridine in the current case), furthermore, the overall void space in the resultant 3D nano-assemblies can be tailored. In addition to the role of spacer, functional groups or elements can also be introduced to the intercalants to engineer the materials functionality. By controlling reaction ambience, in fact, chemical and structural properties can be further modified. With the powder XRD technique, we have observed a lattice expansion of 3.0±0.2% (note the peak shift of $(011)_\beta$, Figure 4b) along [011] of β-MoO_3 generated under nitrogen atmosphere at 350−380 °C; the expansion can be attributed to the trapping of decomposed species in the resulting β-MoO_3 crystal lattice, which has been supported with our FTIR results (see Supporting Information).

There have been many inorganic−organic hybrids that comprise MoO_3 and organic intercalants (e.g., ligands and polymers).[6,7] In principle, this class of materials can be utilized as "green compacts" for nanostrucuted MoO_3 synthesis. Through a careful search for heating conditions for the molecular-sheet condensation, as demonstrated in this Letter, the present method should also be extendable to other intercalated layered inorganic−organic materials such as layered inorganic−organic hybrids (e.g., vanadium oxide (VO_x)−organic hybrids, and MoS_2-organic-intercalated compounds, etc). Our preliminary results show that this method is also suitable for the self-organization of layered metal−sulfide materials.[7b] There should exist many potential applications of the resultant organized nanostructures.

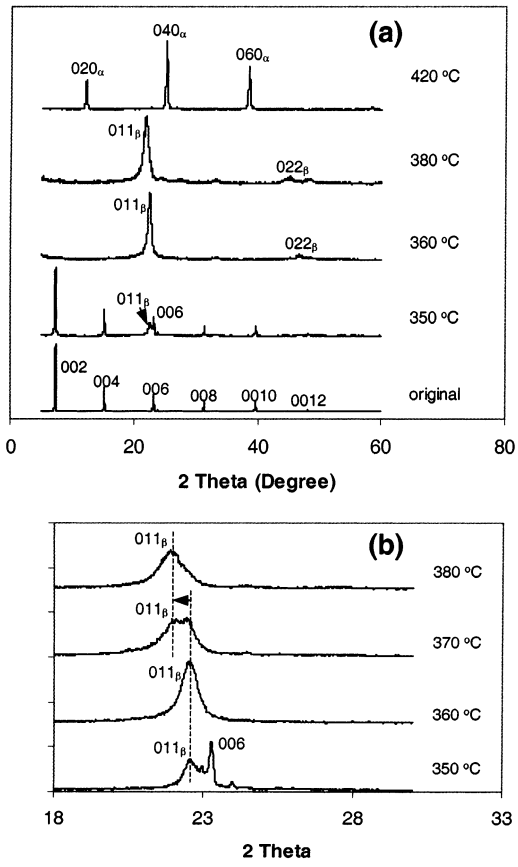

Figure 4. Powder XRD patterns (intensity in arbitrary unit) for samples of MoO_3(4,4′-bipyridyl)$_{0.5}$ crystals (named "original") heated in nitrogen atmosphere at various temperatures: (a) 350, 360, 380, and 420 °C. (b) Detailed diffraction features over 350−380 °C. Nitrogen gas was passed through the reaction tube at 30 mL/min, whose temperature was preset at 50 °C lower than the final temperatures for 1 h (at rising rate 5 °C/min), followed by heat-treatments at 320 °C (preheat temperature at 300 °C), 350, 360, 370, 380, 400, and 420 °C, respectively, for 2 h (at rising rate 0.1 °C/min).

For example, oriented nano-platelets would allow a more efficient intercalation process, since intercalants can enter the MoO_3 host more easily from the sidewalls.[12] Regarding the catalytic reactions, on the other hand, the parallel platelet-morphology may reduce the reaction flow resistance, especially for microreactor systems where the fluid stream stability is crucial.

In summary, inorganic−organic layered hybrid MoO_3-(4,4′-bipyridyl)$_{0.5}$ single-crystals can be utilized as a novel precursor for large-scale organizations of two-dimensional nanostructured MoO_3 platelets within a large predefined space (the nano-assemblies can have a dimension as large as 50−250 μm in the current case). The important synthetic parameters are slow-heating and reaction-atmosphere selection. Precise control over thermal reactions will generate various stacking fashions among the oxide molecular sheets with a desired crystal phase.

Acknowledgment. The authors gratefully acknowledge the financial support of the Ministry of Education and the National Science and Technology Board, Singapore.

Supporting Information Available: SEM images of the sample heated in nitrogen atmosphere. Two FTIR spectra demonstrating the effects of heating atmospheres on the retention of included organic species in the resultant solid MoO_3. This material is available free of charge via the Internet at http://pubs.acs.org.

References and Notes

(1) (a) Ozin, G. A. *Adv. Mater*. **1992**, *4*, 612 and references therein. (b) Zach, M. P.; Ng, K. H.; Penner, R. M. *Science* **2000**, *290*, 2120. (c) Kobayashi, S.; Hamasaki, N.; Suzuki, M.; Kimura, M.; Shirai, H.; Hanabusa, K. *J. Am. Chem. Soc*. **2002**, *124*, 6550. (d) Wang, X.; Li, Y. *J. Am. Chem. Soc*. **2002**, *124*, 2880. (e) Sampanthar, J. T.; Zeng, H. C. *J. Am. Chem. Soc*. **2002**, *124*, 6668. (f) Lou, X. W.; Zeng, H. C. *J. Am. Chem. Soc*. **2003**, *125*. In press.

(2) (a) Moller, K.; Bein, T. *Chem. Mater*. **1998**, *10*, 2950, and references therein. (b) Ying, J. Y.; Mehnert, C. P.; Wong, M. S. *Angew. Chem., Int. Ed*. **1999**, *38*, 56 and the references therein. (c) Thomas, J. M. *Angew. Chem., Int. Ed*. **1999**, *38*, 3588 and references therein.

(3) Thalladi, V. R.; Whitesides, G. M. *J. Am. Chem. Soc*. **2002**, *124*, 3520.

(4) (a) Spahr, M. E.; Bitterli, P.; Nesper, R.; Müller, M.; Krumeich, F.; Nissen, H.-U. *Angew. Chem., Int. Ed. Engl*. **1998**, *37*, 1263. (b) Krumeich, F.; Muhr, H.-J.; Niederberger, M.; Bieri, F.; Schnyder, B.; Nesper, R. *J. Am. Chem. Soc*. **1999**, *121*, 8324. (c) Muhr, H.-J.; Krumeich, F.; Schönholzer, U. P.; Bieri, F.; Niederberger, M.; Gauckler, L. J.; Nesper, R. *Adv. Mater*. **2000**, *12*, 231. (d) Niederberger, M.; Krumeich, F.; Muhr, H.-J.; Müller, M.; Nesper, R. *J. Mater. Chem*. **2001**, *11*, 1941.

(5) "Green compact" (or "ceramic green body") is a term used in ceramic object processing. It refers to a particular ceramic shape prepared from a dry ceramic powder, or a suspension of ceramic powders in a solvent solution, or a paste of a ceramic powder in a limited amount of solvent solution. The basic shape of a green compact is maintained after the subsequent steps of drying, binder burnout, and firing treatment. For more details, see Ring, T. A. *Fundamental of Ceramic Powder Processing and Synthesis*; Academic Press: San Diego, 1996; Chapter 13, p 609.

(6) Hagrman, P. J.; LaDuca, R. L., Jr.; Koo, H. J.; Rarig, R., Jr.; Haushalter, R. C.; Whangbo, M. H.; Zubieta, J. *Inorg. Chem*. **2000**, *39*, 4311.

(7) (a) Wei, X. M.; Zeng, H. C. *Chem. Mater*. **2003**, *15*, 433. (b) Wei, X. M.; Zeng, H. C. In preparation.

(8) Carcia, P. F.; McCarron, E. M., III *Thin Solid Films* **1987**, *155*, 53.

(9) Haber, J.; Lalik, E. *Catal. Today* **1997**, *33*, 119.

(10) Wang, J.; Rose, K. C.; Lieber, C. M. *J. Phys. Chem. B* **1999**, *103*, 8405.

(11) Queeney, K. T.; Friend, C. M. *J. Phys. Chem. B* **2000**, *104*, 409.

(12) (a) Zeng, H. C.; Ng, W. K.; Cheong, L. H.; Xie, F.; Xu, R. *J. Phys. Chem. B* **2001**, *105*, 7178. (b) Zeng, H. C.; Xie, F.; Wong, K. C.; Mitchell, K. A. R. *Chem. Mater*. **2002**, *14*, 1788.